

Diffusion-weighted MR imaging in gynecologic cancers

Shigenobu Motoshima¹, Hiroyuki Irie², Takahiko Nakazono³, Toshiharu Kamura⁴, Sho Kudo²

¹Department of Radiology, Takagi Hospital, Okawa, ²Department of Radiology, Saga University Faculty of Medicine, Saga,

³Department of Radiology, Saga Social Insurance Hospital, Saga, ⁴Department of Obstetrics and Gynecology, Kurume University School of Medicine, Kurume, Japan

Diffusion-weighted imaging (DWI) reflects changes in proton mobility caused by pathological alterations of tissue cellularity, cellular membrane integrity, extracellular space perfusion, and fluid viscosity. Functional imaging is becoming increasingly important in the evaluation of cancer patients because of the limitations of morphologic imaging. DWI is being applied to the detection and characterization of tumors and the evaluation of treatment response in patients with cancer. The advantages of DWI include its cost-effectiveness and brevity of execution, its complete noninvasiveness, its lack of ionizing radiation, and the fact that it does not require injection of contrast material, thus enabling its use in patients with renal dysfunction. In this article, we describe the clinical application of DWI to gynecological disorders and its diagnostic efficacy therein.

Keywords: Diagnosis, Diffusion magnetic resonance imaging, Gynecology, Magnetic resonance imaging, Neoplasms

INTRODUCTION

Diffusion-weighted imaging (DWI) visualizes the random microscopic mobility of water (Brownian motion) and thereby provides a tissue contrast that is different from that made with conventional T1-weighted (T1WI) and T2-weighted imaging (T2WI) [1-4]. DWI reflects changes in proton mobility caused by the alteration of tissue cellularity and the integrity of the cellular membrane, tortuosity of extracellular space, and viscosity of fluids due to pathologic processes [4-6]. Altering the gradient amplitude, duration, and time interval (b-value, measured in seconds per square millimeter) between paired diffusion gradients alters the sensitivity to the degree of water motion [7,8]. A higher b-value (b=e.g., 800 or 1,000 sec/mm²) has been recommended for the female pelvic region because it results in more diffusion weighting with better background

suppression [1,4,8]. By performing DWI using different b-values, quantitative analysis, namely, the calculation of apparent diffusion coefficient (ADC) values, is possible and the ADC values can be displayed as a parametric map (ADC map) [8]. Restricted water diffusion demonstrates high signal intensity on DWI and lower ADC values on ADC map [1,7,8].

DWI was at first used in central nervous system imaging, especially in cases of acute ischemic stroke which causes a decrease of water diffusion compared with that of normal tissue [3]. DWI has been shown to be capable of detecting early or subtle changes within the brain before any visible abnormality appears on conventional imaging [8]. DWI has been prone to severe motion sensitivity due to the long scan times, because this will limit the effects of patient motion artifacts [9]. However, recent developments in fast magnetic resonance image (MRI) techniques have helped to overcome the difficulties, respiratory and bowel peristaltic motion, of abdominal and pelvic DWI and have increased the role and potential of MRI in evaluating the abdomen and pelvis [1]. Although performing DWI in the body is challenging because the inhomogeneity of the magnetic field over a large imaging area and susceptibility to motion artifacts related to respiratory and bowel peristaltic

Received Aug 22, 2011, Revised Nov 6, 2011, Accepted Nov 16, 2011

Correspondence to Shigenobu Motoshima

Department of Radiology, Takagi Hospital, 141-11 Sakemi, Okawa 8310016, Japan. Tel: 81-944-87-0001, Fax: 81-944-87-9310, E-mail: s.motoshima@gmail.com

Copyright © 2011. Asian Society of Gynecologic Oncology, Korean Society of Gynecologic Oncology

This is an Open Access article distributed under the terms of the Creative Commons Attribution Non-Commercial License (<http://creativecommons.org/licenses/by-nc/3.0/>) which permits unrestricted non-commercial use, distribution, and reproduction in any medium, provided the original work is properly cited.

motion arising from different organs conspire to degrade image quality [9,10].

In general, malignant tumors have a higher cellularity than benign tumors; therefore, DWI can assist in differentiating malignant from benign tumors [11]. DWI is presently used for tumor detection, tumor characterization, and the evaluation of treatment response in patients with cancer [8]. Recent studies have described the usefulness of DWI for detecting malignant tumors of the liver, renal, prostate, colorectal, and pancreas [12-39]. Moreover, a quantitative analysis of ADC values can be used to characterize tumors and assess responses to treatment [40-45]. Other advantages of DWI include its cost-effectiveness and brevity of execution, its complete non-invasiveness, its lack of ionizing radiation, and the fact that no injection of contrast material is required [2,46-48].

In this article, we describe the clinical application of DWI in gynecological disorders and its diagnostic role therein. We used a DWI with a high b-value of 0 and 1,000 sec/mm² and a reversed black-and-white gray scale.

DWI OF NORMAL FEMALE REPRODUCTIVE ORGANS

Normal structures, such as the premenopausal uterine endometrium and ovarian mesenchyme, excluding ovarian follicular cysts, show high signal intensity on DWI [49,50]. Interestingly, Kido et al. [51] observed cyclical changes in ADC values in the normal uterus during different menstrual phases in healthy reproductive age females. For the myometrium and endometrium, the mean ADC values tended to be lower in the menstrual phase than in other phases. The utility of DWI for detecting ectopically located abnormal gonads has been reported [4]. Normal or reactive lymph nodes and bowel mucosa are also hyperintense on DWI of the female pelvic cavity [7].

TUMOR DETECTION

On DWI, background tissues are relatively suppressed, whereas most forms of tumors show restricted water diffusion, which results in moderate to marked tumor conspicuity [1]. DWI may depict small-volume tumors which are not easily detectable by conventional imaging modalities [1]. Restricted water diffusion is generally considered associated with malignant tumors as a result of high cellularity [11]. Clinicians interpreting DWI in the abdominal and pelvic regions, however, should keep in mind that the likelihood that a lesion with restricted water diffusion is a benign disease was as high as 22% and that lesion with restricted water diffusion are much

more likely to be malignant in patients with known malignant disease [52].

Namimoto et al. [47] showed a decision-making diagram in the MRI diagnosis of gynecological disorders with the addition of DWI and ADC values. ADC values may make it possible to differentiate between normal and cancerous tissues in the uterine cervix and endometrium, with cut-off ADC values of 1.4×10^{-3} mm²/sec and 1.15×10^{-3} mm²/sec, respectively. Among cystic ovarian lesions, most benign endometrial cysts and mature cystic teratomas had lower ADC values than malignant neoplasms, with cut-off ADC values of 2.0×10^{-3} mm²/sec. Detection of high signal intensity on DWI may be useful for evaluation of peritoneal dissemination.

The ADC values may vary on acquisition parameters associated with b-values, magnetic field strength (3.0 T vs. 1.5 T), and breath-holding technique [53]. Thus absolute quantification is hampered by the fact that ADC values are influenced by all of these technical factors.

Due to the relatively poor spatial resolution of DWI, it is difficult to define the anatomic location of the abnormal signal on DWI, especially in small lesions, such as peritoneal implants or small recurrence or lymph node metastasis. One can resolve this problem by using recently developed fusion software that can automatically overlay the DWI onto conventional MRI. Even without the fusion software, one can correlate the location of signal on the DWI with conventional MRI [4].

1. Gynecological malignant tumors

Cervical cancer has demonstrated significantly lower ADC values than normal cervical tissues [1,6,46,47,54]. Moreover, according to Liu et al. [55], squamous cell carcinoma of the uterine cervix tends to demonstrate lower ADC values than adenocarcinoma, providing a means to predict the histologic type of uterine cervical cancer to some extent. Similar findings to cervical cancers have been noted in endometrial cancers (Fig. 1), with a tendency toward lower ADC values in higher-grade lesions [1,3,6,47,49].

2. Peritoneal dissemination

The peritoneal cavity is a common site of metastatic spread for gynecological malignant tumors, especially ovarian cancer [2,56-58]. On DWI, ascites and most bowel contents have suppressed signal intensity, while peritoneal dissemination involving the bowel shows high signal intensity [57]. Thus increasing the conspicuity of the dissemination site, DWI has a high accuracy at detecting peritoneal dissemination [56,57]. Sensitivity and specificity of depicting peritoneal dissemination with the combination of DWI and conventional MRI, DWI alone, and conventional MRI alone were reported as 84% and

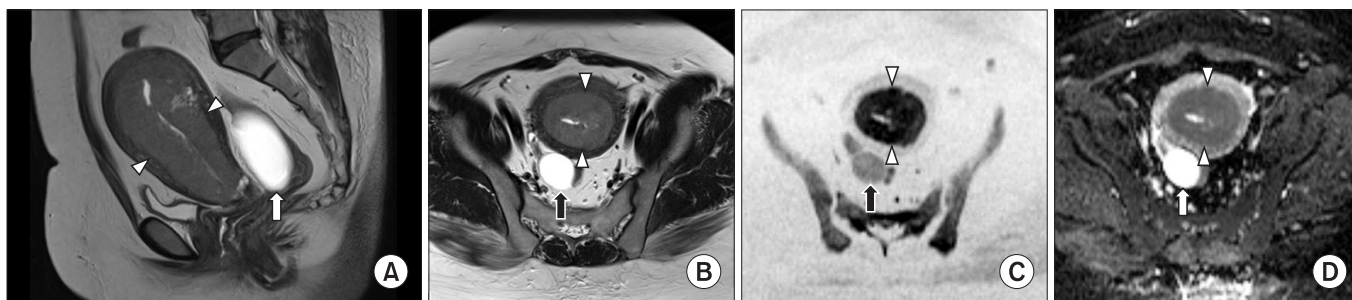


Fig. 1. Stage IC endometrioid adenocarcinoma grade 1 (G1) of the endometrium in a 30-year-old woman. The tumor (arrowheads) shows slightly high signal intensity on sagittal and axial T2-weighted imaging (A, B) and high signal intensity on axial diffusion-weighted imaging (C). Axial apparent diffusion coefficient (ADC) map (D) demonstrated low ADC values (0.75×10^{-3} mm²/sec). Arrow, right hydrosalpinx.

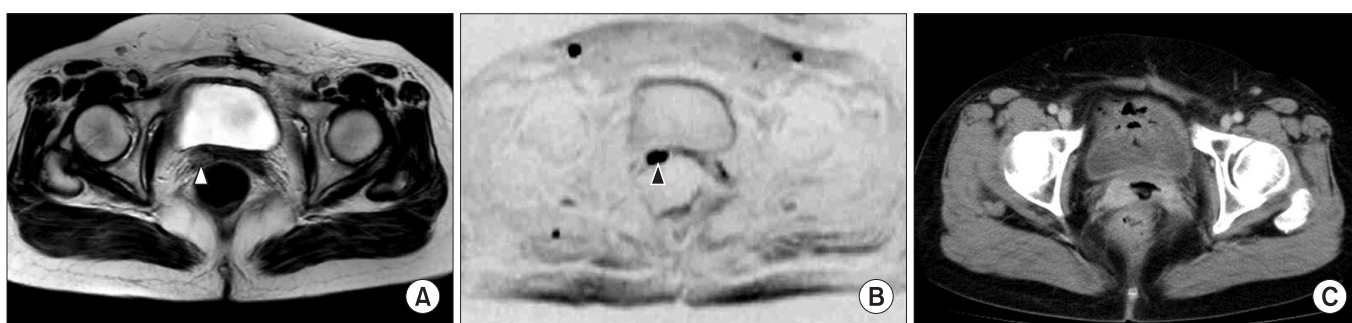


Fig. 2. Postoperative vaginal cuff recurrence of stage IVB endometrial carcinoma in a 66-year-old woman. Axial T2-weighted imaging shows a slightly high-signal lesion (arrowhead) on the right side of vaginal cuff (A). Axial diffusion-weighted imaging clearly depicts the lesion (B) and the apparent diffusion coefficient (ADC) map (not shown) demonstrated low ADC values (0.91×10^{-3} mm²/sec). The lesion is difficult to distinguish on contrast-enhanced-computed tomography (C).

91%, 71% and 90%, 52% and 92%, respectively [56].

3. Recurrent disease

As with the case of peritoneal dissemination, DWI may be also useful in depicting small recurrent disease, such as in the vaginal cuff site (Fig. 2). Small recurrent disease, covered by the serosal surface of intestinal loops and solid viscera are difficult to detect with computed tomography (CT) or conventional MRI, because they are masked by the similarity of their attenuation or signal intensity to that of adjacent structures [50].

4. Lymph node staging

Evaluation of pelvic lymph node status is important in devising a treatment plan in gynecologic malignant tumors. The differentiation between benign and malignant nodes in the pelvic cavity remains challenging for imaging, because the morphological criteria including size, shape or presence of necrosis, has so far not been absolutely reliable with enlarged reactive lymph nodes and malignant non-enlarged lymph nodes [59-62].

Diagnoses of lymph node pathology by conventional MRI and CT are based on roughly defined size and morphologic

criteria. The sensitivities for conventional MRI or CT in detecting lymph node metastases in gynecologic malignant tumors range from 43% to 73% [63,64]. Some reports have demonstrated the usefulness of DWI and ADC values in the detection of metastatic lymph nodes in gynecological malignant tumors [61,65,66].

Lin et al. [65] evaluated for detection of pelvic lymph node metastasis in patients with cervical and endometrial cancers on DWI. The combination of size and relative ADC values was useful compared with conventional MRI in detecting pelvic lymph node metastasis in patients with cervical and endometrial cancers, and the sensitivity and specificity were 83 and 25% with cervical cancer, 99 and 98% with endometrial cancer, respectively [65]. Kim et al. [61] reported the ADC values were significantly lower in the metastatic lymph nodes than in the nonmetastatic lymph nodes of cervical cancer patients, and the area-under-the-curve of ADC values for differentiating metastatic from nonmetastatic lymph nodes was 0.902×10^{-3} mm²/sec. With this threshold, the sensitivity and specificity of ADC values for differentiating metastatic from nonmetastatic lymph nodes were 87% and 80%, respectively. Measurement of ADC values may be useful, especially for detection of small

metastatic lymph nodes compared with the limited sensitivity of CT and conventional MRI [59,61]. DWI shows relatively poor anatomical detail, fusion of DWI with T2WI improves identification of pelvic lymph nodes and their metastases [7,59,60,67]. On the contrary, some reports showed that the role of DWI and ADC values in distinguishing benign and malignant lymph nodes is limited [7,50,59,68], because cellular tissues such as lymph nodes have high signal intensity on DWI regardless of their biologic behavior [60,69]. There is still considerable overlap, however, in ADC values, and lymph node evaluation in clinical practice has to continue to rely on conventional features such as shape, size, and growth patterns [52].

LESION CHARACTERIZATION

Differences in tumor cellularity may reflect their histologic composition and biologic aggressiveness [8]. Additional information obtained from a quantitative analysis of ADC values can be used to characterize tumors [6]. However, there are some difficulties due to the considerable overlap in ADC values of benign and malignant tumors [8]. Even in malignant tumor necrosis, edema or cystic components show increased water diffusion due to the decrease in tumor cellularity. Therefore, interpretation of DWI requires consideration of the pa-

tient's clinical presentation and history, as well as a morphological assessment by conventional MRI [1].

1. Uterine myometrial lesion

As pathological evaluation of uterine myometrial lesions is difficult, imaging diagnosis is important. However, since uterine sarcomas are occasionally associated with various types of degeneration or cellular histologic subtypes, strict differentiation of benign and malignant myometrial tumors on the basis of MRI findings may be difficult [47,70]. Tamai et al. [71] reported that DWI may be an additional tool for distinguishing uterine sarcomas from benign leiomyomas (Fig. 3); however, the ADC values overlap with those of ordinary leiomyomas and cellular leiomyomas.

2. Tumors in the uterine endometrial cavity

ADC values provide useful information in differentiating malignant (endometrial carcinoma and carcinosarcoma) from benign (submucosal leiomyoma and endometrial polyp) endometrial cavity lesions [71].

3. Adnexal lesions

An ovarian mass with a solid component was classically predictive of a malignant tumor [72]. However, many benign ovarian masses can display a solid component including fibro-

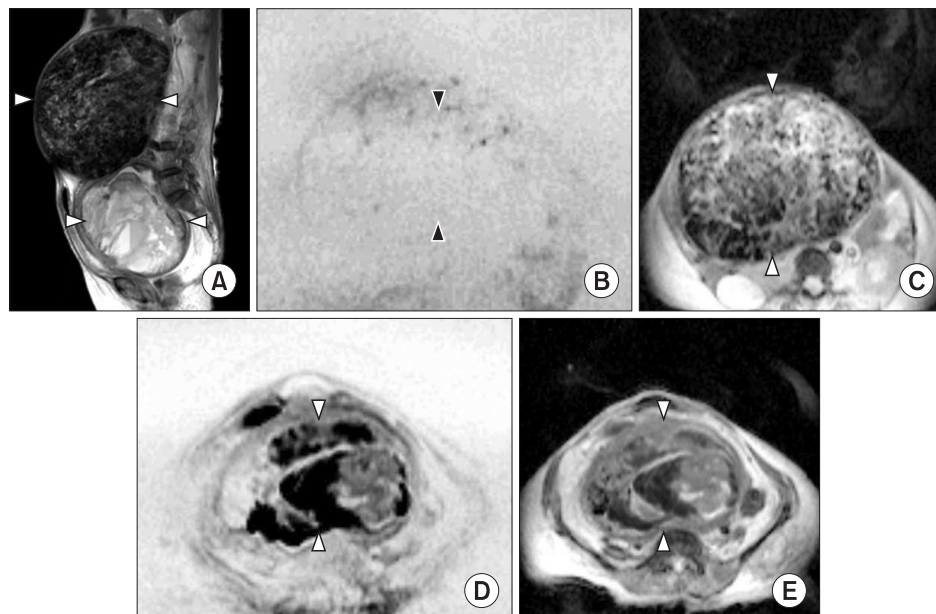


Fig. 3. Uterine leiomyosarcoma and leiomyoma in a 72-year-old woman. Sagittal T2-weighted imaging shows an enlarged uterus with two solid lesions (arrowheads) (A). The upper lesion (arrowheads) shows low signal intensity on axial diffusion-weighted imaging (DWI) (B) and the apparent diffusion coefficient (ADC) map (C) demonstrated high ADC values ($2.13 \times 10^{-3} \text{ mm}^2/\text{sec}$). The lower lesion (arrowheads) shows high signal intensity on axial DWI (D) and the ADC map (E) demonstrated low ADC values ($0.67 \times 10^{-3} \text{ mm}^2/\text{sec}$). Pathological examination revealed leiomyoma in the upper lesion and leiomyosarcoma in the lower lesion.

mas, cystadenofibromas, Brenner tumors, sclerosing stromal tumors, and theca cell tumors. The addition of DWI improved the MR characterization of complex adnexal masses compared with conventional MRI alone; indeed, DWI has recently been shown to be effective in the differentiation of benign from malignant adnexal masses [73,74]. Therefore, a solid component in an adnexal mass with a high signal intensity on DWI is predictive of malignant tumors (Fig. 4) [4,74,75]. According to Takeuchi et al. [75], the mean ADC values between the benign and malignant ovarian tumors differed significantly. Using a cutoff ADC value of $1.15 \times 10^{-3} \text{ mm}^2/\text{sec}$, differentiating benign from malignant/borderline malignant lesions had a sensitivity of 74%, specificity of 80%, positive predictive value (PPV) of 94%, and negative predictive value (NPV) of 44%. Using a cutoff ADC value of $1.0 \times 10^{-3} \text{ mm}^2/\text{sec}$, differentiating benign from malignant/borderline malignant lesions had a sensitivity of 46%, specificity of 100%, PPV of 100%, and NPV of 32%. However, there were some overlaps between the mean ADC values of the malignant and benign ovarian lesions. They

considered that their results may reflect the increased mean ADC values in some malignant lesions owing to the existence of small necrotic or cystic areas in solid tumoral components, or fluid collection intervening papillary projections, and the decreased mean ADC values in some benign lesions owing to relative hypercellularity in functioning ovarian tumors such as thecomas, or restriction of the water diffusion by dense stromal proliferation in fibroma without edematous changes [75]. In addition, a study by Thomassin-Naggara et al. [74] showed that a solid component that exhibits low signal intensity on both T2WI and DWI was always benign (Fig. 5). Some reports showed that ADC values may provide limited information in the differential diagnosis of a cystic ovarian tumor [76,77]. Due to the morphological and histological variety of ovarian tumors, DWI may have a role in the preoperative evaluation of ovarian tumors. This is also useful to determine operative strategy, including the planning of the operation method, expectant management, or possibility and the feasibility of laparoscopy and conservative surgery [74]. However, accord-

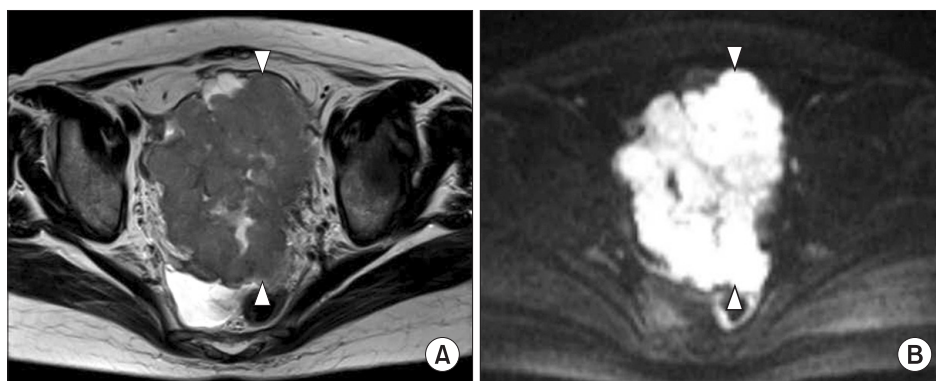


Fig. 4. Stage IV serous papillary adenocarcinoma of right ovary in a 60-year-old-woman. MR images show huge lobulated, solid lesion (arrowheads) dorsal to the uterus. The lesion shows slightly low signal intensity on axial T2-weighted imaging (A) and very high signal intensity on axial (original) diffusion-weighted imaging (B). Apparent diffusion coefficient map (not shown) demonstrated low ADC values ($0.75 \times 10^{-3} \text{ mm}^2/\text{sec}$).

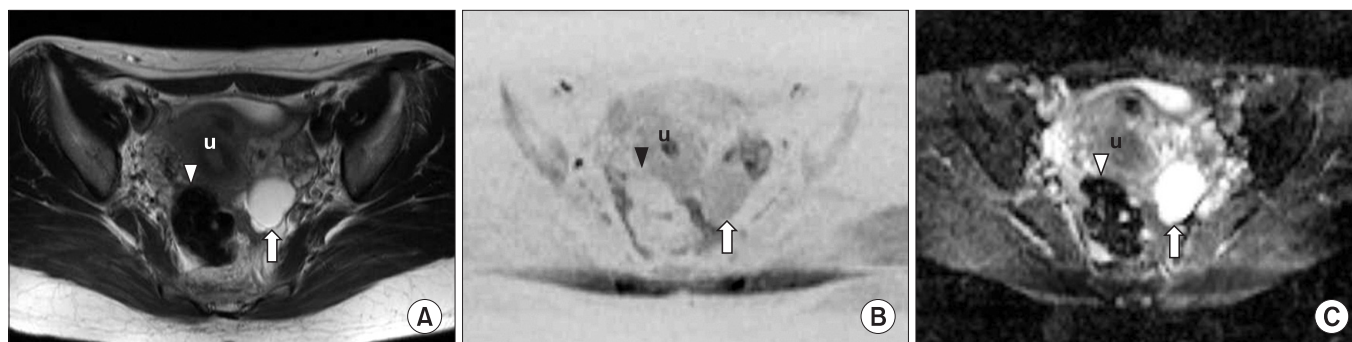


Fig. 5. Right ovarian fibroma in a 37-year-old woman. MR images show lobulated, solid lesion (arrowhead) in the right adnexal region. The lesion shows low signal on axial T2-weighted imaging (A) and diffusion-weighted imaging (B). Apparent diffusion coefficient map (C) shows low values ($0.96 \times 10^{-3} \text{ mm}^2/\text{sec}$), which is representing T2 blackout effect. U, uterus; arrow, right paraovarian cyst.

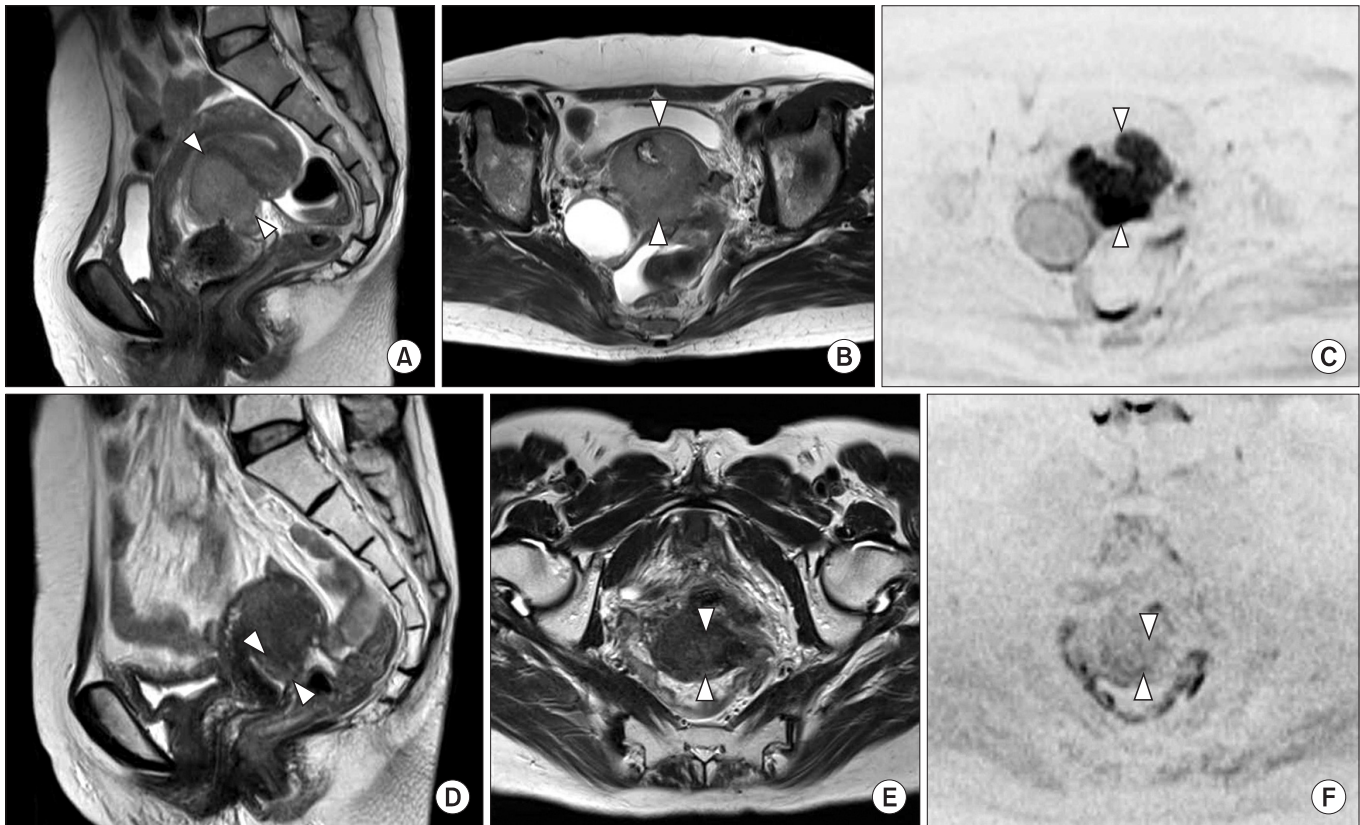


Fig. 6. Stage IIA squamous cell carcinoma of the cervix in a 54-year-old woman. Posterior lip of the cervix (arrowheads) shows high signal intensity on sagittal and axial T2-weighted imaging (T2WI) (A, B) and axial diffusion-weighted imaging (DWI) (C). The apparent diffusion coefficient (ADC) map (not shown) demonstrated low ADC values ($0.72 \times 10^{-3} \text{ mm}^2/\text{sec}$). The lesion (arrowheads) was reduced and difficult to identify after radiation therapy on sagittal and axial T2WI (D, E) and signal intensity was decreased on axial DWI (F). ADC values increased to $1.34 \times 10^{-3} \text{ mm}^2/\text{sec}$ (not shown).

ing to Namimoto et al. [47], ADC values varied widely among malignant ovarian tumors, a phenomenon attributable to their morphological and histological variety.

MONITORING TREATMENT RESPONSE

DWI shows promise as a biomarker for tumor treatment responses [1,2,7,47,78-80]. Increases in ADC values would reflect an increase in the mobility of water, either through the loss of membrane integrity or a change in the relative volume of extracellular space with a corresponding decrease in cellular size or number, as seen with necrosis or apoptosis due to tumor treatment (Fig. 6) [78,81]. In short, this approach is based on early cellular changes in the tumor on initiation of effective chemotherapy or radiation therapy [52]. Furthermore, treatment effects can be observed within the first 24 hours after initiating treatment due to cell swelling, which results in a transient decrease in ADC values [8]. In tumor treatment, the change in ADC values accurately reflected a change in

cellularity and could be measured earlier than changes in tumor volume, and ADC values have been used to characterize tumors and quantify treatment-induced changes, which may occur earlier than conventional morphologic alterations [78,80,82-86]. A recent study evaluated ADC histograms in the prediction of chemotherapy response in patients with metastatic ovarian or primary peritoneal cancer [80]. The study indicated that an early increase of ADC values and later decrease of histogram skew and kurtosis can detect chemotherapy response assessed with integrated morphologic (size reduction) and biochemical (serum CA-125 level) criteria. Several studies have shown that cellular tumors with low baseline pretreatment ADC values responded better to chemotherapy or radiation treatment than tumors with high pretreatment ADC values [87-89]. One possible explanation is that necrotic tumors, which exhibit higher ADC values, are frequently hypoxic, acidotic, and poorly perfused, leading to diminished sensitivity to chemotherapy and radiation therapy [8].

WHOLE-BODY DWI

Whole-body DWI was first reported in 2004 by Takahara et al. [69], and constituted a unique concept, called “diffusion-weighted whole-body imaging with background body signal suppression” (DWIBS) [90]. Potential clinical applications of whole-body DWI include cancer staging because both the primary tumor and distant metastases demonstrate restricted water diffusion [1,90]. Accordingly, whole-body DWI has the potential for use in tumor staging, detecting responses to cancer therapy, and detecting tumor persistence or recurrence [90]. Three-dimensional (3D) display of DWI with a reversed black-and-white gray scale can produce positron emission tomography (PET)-like images (Fig. 7) [4,91].

Komori et al. [92] reported that a larger number of malignant tumors were detected visually with whole-body DWI than with PET/CT. However, according to Satoh et al. [93], PET/CT proved to be more reliable than DWI and contrast-enhanced CT (CE-CT) in the detection of peritoneal dissemination. The sensitivity of PET/CT, DWI, and CE-CT were 94%, 85%, and 83% and the specificity were 94%, 89%, and 87%, respectively [93]. Nevertheless, DWI may still be of value because it showed satisfactory sensitivity for lesions and can be used as a screening tool because of its excellent lesion specificity [93]. The advantages of DWI compared with PET/CT include its noninvasiveness and relatively low cost [93]. However, whole-body DWI does have several limitations [90]. First, whole-body DWI does

not exclusively visualize malignant tumors, as benign pathologies with restricted water diffusion such as abscesses also exhibit high signal intensity on whole-body DWI [90]. Second, whole-body DWI also visualizes numerous normal structures; namely, the brain, salivary glands, tonsils, spleen, gallbladder, small intestine/small intestinal contents, colon, adrenal glands, prostate, testes, penis, spinal cord, peripheral nerves, lymph nodes, bone marrow, endometrium and ovaries may all exhibit high signal intensity [90]. Another limitation is the lack of sufficient anatomical information [90]. According to Low [1], whole-body DWI seems unlikely to entirely replace PET/CT, because whole-body DWI does not provide true metabolic information. Low [1] advocated that initial evaluation with PET/CT might be used to identify sites of primary and metastatic tumor, and follow-up whole-body DWI could be performed to monitor the tumor response to therapy.

PITFALLS

1. T2 shine-through effect

One of the pitfalls of visual assessment of DWI is known as the T2 shine-through effect [8]. Because the signal intensity on DWI can be influenced by the signal intensity on T2WI, high signal intensity tissues on T2WI may exhibit increased signal intensity on DWI [47]. ADC map eliminates the effect of T2 decay. In cases of high signal intensity on DWI, evaluation of T2WI as well as an ADC map, which depicts changes in signal intensity that are solely caused by diffusion, are required [1].

2. T2 blackout effect

A T2 blackout effect occurs when there is low or very low signal intensity of the solid component on T2WI and due to high collagen concentration and low cellularity [74]. Accordingly, low ADC values may be misinterpreted as a malignancy, and concurrent evaluation of DWI may be necessary (Fig. 5).

3. Ovarian cystic lesions with water diffusion restriction

DWI is useful for tumor characterization, namely differentiating malignant and benign lesions. However, abscesses, mature cystic teratomas, and hemorrhagic cysts such as endometriotic cysts may show high signal intensity on DWI and lower ADC values than other benign ovarian cysts [47,94-96]. Water diffusion in abscesses is restricted due to the paramagnetic properties of cystic components. In the majority of mature cystic teratomas, conventional MRI with fat saturation may be sufficient for making a correct diagnosis [76]. According to Nakayama et al. [76], mature cystic teratomas are lined with a keratinized squamous epithelium in most cases; by contrast,

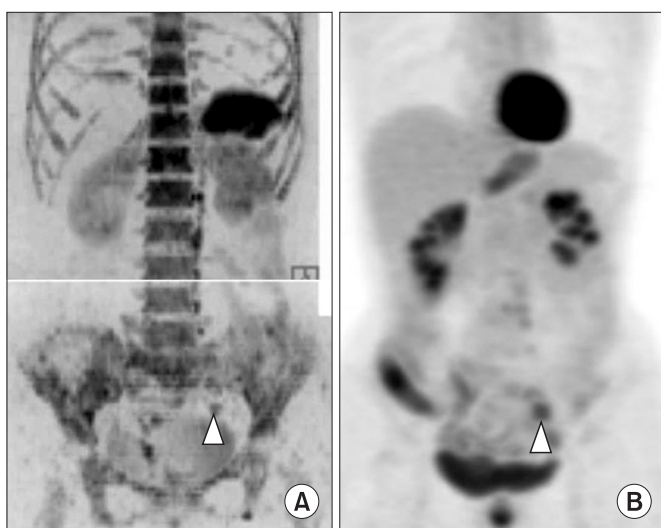


Fig. 7. Left common iliac lymph node metastasis posttreatment (operation and subsequent chemotherapy) of stage IC endometrial carcinoma in a 70-year-old woman. Left common iliac lymph node region (arrowhead) shows high signal intensity on inverted grayscale of diffusion-weighted imaging (A). Positron emission tomography also shows abnormal uptake in the left common iliac lymph node region (arrowhead) (B).

fatty components and calcification are pathologically found in 67-75%. Keratinoid substances restrict water diffusion in mature cystic teratomas [76]. DWI and ADC values may be useful and serve as an adjunctive tool to ensure the accuracy of the diagnosis, particularly in patients with a teratoma with paucity of fat (Fig. 8) [76]. Endometriotic cysts tend to contain hemoglobin degeneration products, and its viscosity lowers ADC values [47]. On the contrary, detection of a malignant lesion, such as malignant transformation of a mature cystic teratoma or a malignant tumor arising in an endometriotic cyst, might be difficult, because the entire cystic component may show high signal intensity on DWI.

4. Inflammatory lesion

A solid adnexal mass with high signal intensity on DWI within a solid component is predictive of malignancy, as mentioned above. Inflammatory, granulomatous adnexal lesions may show morphologically solid and restricted water diffusion on MRI and can mimic a malignant tumor (Fig. 9). Oussalah

et al. [97] reported restricted water diffusion in the inflamed bowel of a Crohn's disease patient; this restricted water diffusion in active Crohn's disease is explained by the strong association with lymphoid aggregates.

5. Well-differentiated malignant tumors

In poorly differentiated malignant tumors, the extracellular space is characterized by increased tortuosity, with a resultant decrease in ADC values, whereas well-differentiated malignant tumors (particularly adenocarcinomas) may not show high signal intensity on DWI or low ADC values [2,7,49,67].

CONTROVERSY

In gynecologic disorders, conventional morphologic evaluation on T1WI and T2WI is essential. DWI should be utilized as a complementary sequence to conventional morphologic imaging. Because DWI has relatively poor spatial resolution,



Fig. 8. Right ovarian teratoma with paucity of fat in a 77-year-old woman. The cystic lesion (arrowheads) shows high signal intensity on axial T2-weighted imaging (A) and axial diffusion-weighted imaging (C) in the right adnexal region. The apparent diffusion coefficient (ADC) map (not shown) demonstrated low ADC values ($0.67 \times 10^{-3} \text{ mm}^2/\text{sec}$). A small fraction of the cystic lesion shows high signal intensity (arrows) on axial T1-weighted (B), and chemical shift imaging (not shown) suggested fat. H&E stain (not shown) indicated hyperkeratotic epidermis cells. u, uterus.

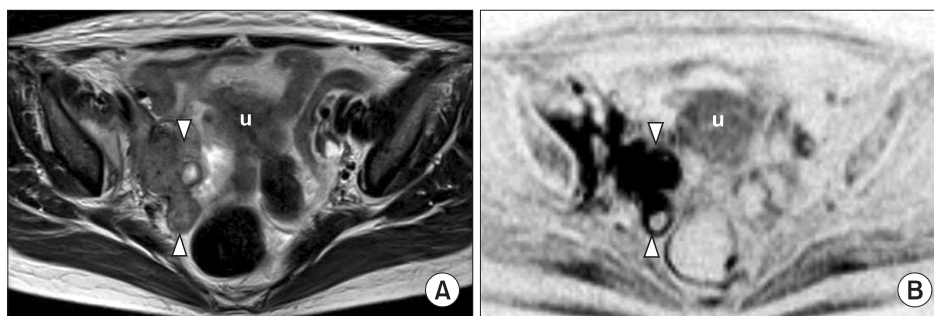


Fig. 9. Right salpingo-oophoritis in a 50-year-old woman. Axial T2-weighted imaging show solid lesion (arrowheads) in the right adnexal region (A). Fat saturated contrast enhanced (FS-CE) T1-weighted (not shown) was homogeneously enhanced. The solid lesion shows high signal intensity on axial diffusion-weighted imaging (B) and the apparent diffusion coefficient (ADC) map (not shown) demonstrated low ADC values ($0.84 \times 10^{-3} \text{ mm}^2/\text{sec}$). Pathological diagnosis was a right salpingo-oophoritis. u, uterus.

detection of small lesions on DWI may be limited. It is necessary to refer to other imaging sequences or fusion images for sufficient identification of lesion boundaries [47]. Moreover, a major challenge to the widespread implementation of DWI is the lack of an acceptable standard approach to data collection and analysis [8,56]. Standardization will allow for improved repeatability and reproducibility based on diffusion indices [2]. Reproducible measurements are particularly important to determine both the limits of using quantitative ADC values to discern the magnitude of change and whether DWI measurements are to be routinely used for monitoring therapeutic effects [8].

CONCLUSION

Functional imaging is becoming increasingly important in the evaluation of cancer patients because of the limitations of morphologic imaging [1]. DWI can be applied widely for tumor detection and tumor characterization and for the monitoring of response to treatment [47]. However, since there are some overlaps on DWI between benign and malignant gynecological disease, DWI evaluation of the lesion should be done in concert with conventional imaging, to distinguish between benign and malignant gynecological disorders [47]. The advantages of DWI include its cost-effectiveness and brevity of execution, its complete noninvasiveness, its lack of ionizing radiation, and the fact that it does not require injection of contrast material, thus enabling its use in patients with reduced renal function [2,8,47,48]. DWI could provide supplemental information in patients with gynecological disorders and could easily be incorporated into standard clinical protocols utilizing MRI [47,78,90].

CONFLICT OF INTEREST

No potential conflicts of interest relevant to this article were reported.

REFERENCES

1. Low RN. Diffusion-weighted MR imaging for whole body metastatic disease and lymphadenopathy. *Magn Reson Imaging Clin N Am* 2009;17:245-61.
2. Padhani AR, Liu G, Koh DM, Chenevert TL, Thoeny HC, Takahara T, et al. Diffusion-weighted magnetic resonance imaging as a cancer biomarker: consensus and recommendations. *Neoplasia* 2009;11:102-25.
3. Inada Y, Matsuki M, Nakai G, Tatsugami F, Tanikake M, Narabayashi I, et al. Body diffusion-weighted MR imaging of uterine endometrial cancer: is it helpful in the detection of cancer in nonenhanced MR imaging? *Eur J Radiol* 2009;70:122-7.
4. Koyama T, Togashi K. Functional MR imaging of the female pelvis. *J Magn Reson Imaging* 2007;25:1101-12.
5. Van Beers BE, Vilgrain V. Biomarkers in abdominal imaging. *Abdom Imaging* 2009;34:663-7.
6. Kilickesmez O, Bayramoglu S, Inci E, Cimilli T, Kayhan A. Quantitative diffusion-weighted magnetic resonance imaging of normal and diseased uterine zones. *Acta Radiol* 2009;50:340-7.
7. Whittaker CS, Coady A, Culver L, Rustin G, Padwick M, Padhani AR. Diffusion-weighted MR imaging of female pelvic tumors: a pictorial review. *Radiographics* 2009;29:759-74.
8. Koh DM, Collins DJ. Diffusion-weighted MRI in the body: applications and challenges in oncology. *AJR Am J Roentgenol* 2007;188:1622-35.
9. Kallehauge JF, Tanderup K, Haack S, Nielsen T, Muren LP, Fokdal L, et al. Apparent Diffusion Coefficient (ADC) as a quantitative parameter in diffusion weighted MR imaging in gynecologic cancer: Dependence on b-values used. *Acta Oncol* 2010;49:1017-22.
10. Koh DM, Takahara T, Imai Y, Collins DJ. Practical aspects of assessing tumors using clinical diffusion-weighted imaging in the body. *Magn Reson Med Sci* 2007;6:211-24.
11. Fujii S, Matsusue E, Kigawa J, Sato S, Kanasaki Y, Nakanishi J, et al. Diagnostic accuracy of the apparent diffusion coefficient in differentiating benign from malignant uterine endometrial cavity lesions: initial results. *Eur Radiol* 2008;18:384-9.
12. Parikh T, Drew SJ, Lee VS, Wong S, Hecht EM, Babb JS, et al. Focal liver lesion detection and characterization with diffusion-weighted MR imaging: comparison with standard breath-hold T2-weighted imaging. *Radiology* 2008;246:812-22.
13. Takeuchi M, Matsuzaki K, Kubo H, Nishitani H. Diffusion-weighted magnetic resonance imaging of urinary epithelial cancer with upper urinary tract obstruction: preliminary results. *Acta Radiol* 2008;49:1195-9.
14. Paudyal B, Paudyal P, Tsushima Y, Oriuchi N, Amanuma M, Miyazaki M, et al. The role of the ADC value in the characterisation of renal carcinoma by diffusion-weighted MRI. *Br J Radiol* 2010;83:336-43.
15. Kilickesmez O, Atilla S, Soylu A, Tasdelen N, Bayramoglu S, Cimilli T, et al. Diffusion-weighted imaging of the

- rectosigmoid colon: preliminary findings. *J Comput Assist Tomogr* 2009;33:863-6.
16. Rao SX, Zeng MS, Chen CZ, Li RC, Zhang SJ, Xu JM, et al. The value of diffusion-weighted imaging in combination with T2-weighted imaging for rectal cancer detection. *Eur J Radiol* 2008;65:299-303.
 17. Hosonuma T, Tozaki M, Ichiba N, Sakuma T, Hayashi D, Yanaga K, et al. Clinical usefulness of diffusion-weighted imaging using low and high b-values to detect rectal cancer. *Magn Reson Med Sci* 2006;5:173-7.
 18. Wang Y, Chen ZE, Nikolaidis P, McCarthy RJ, Merrick L, Sternick LA, et al. Diffusion-weighted magnetic resonance imaging of pancreatic adenocarcinomas: association with histopathology and tumor grade. *J Magn Reson Imaging* 2011;33:136-42.
 19. Kamisawa T, Takuma K, Anjiki H, Egawa N, Hata T, Kurata M, et al. Differentiation of autoimmune pancreatitis from pancreatic cancer by diffusion-weighted MRI. *Am J Gastroenterol* 2010;105:1870-5.
 20. Lemke A, Laun FB, Klauss M, Re TJ, Simon D, Delorme S, et al. Differentiation of pancreas carcinoma from healthy pancreatic tissue using multiple b-values: comparison of apparent diffusion coefficient and intravoxel incoherent motion derived parameters. *Invest Radiol* 2009;44:769-75.
 21. Kartalis N, Lindholm TL, Aspelin P, Permert J, Albiin N. Diffusion-weighted magnetic resonance imaging of pancreas tumours. *Eur Radiol* 2009;19:1981-90.
 22. Fattahi R, Balci NC, Perman WH, Hsueh EC, Alkaade S, Havlioglu N, et al. Pancreatic diffusion-weighted imaging (DWI): comparison between mass-forming focal pancreatitis (FP), pancreatic cancer (PC), and normal pancreas. *J Magn Reson Imaging* 2009;29:350-6.
 23. Ichikawa T, Erturk SM, Motosugi U, Sou H, Iino H, Araki T, et al. High-b value diffusion-weighted MRI for detecting pancreatic adenocarcinoma: preliminary results. *AJR Am J Roentgenol* 2007;188:409-14.
 24. Rosenkrantz AB, Mannelli L, Kong X, Niver BE, Berkman DS, Babb JS, et al. Prostate cancer: utility of fusion of T2-weighted and high b-value diffusion-weighted images for peripheral zone tumor detection and localization. *J Magn Reson Imaging* 2011;34:95-100.
 25. Rosenkrantz AB, Kong X, Niver BE, Berkman DS, Melamed J, Babb JS, et al. Prostate cancer: comparison of tumor visibility on trace diffusion-weighted images and the apparent diffusion coefficient map. *AJR Am J Roentgenol* 2011;196:123-9.
 26. Iwazawa J, Mitani T, Sassa S, Ohue S. Prostate cancer detection with MRI: is dynamic contrast-enhanced imaging necessary in addition to diffusion-weighted imaging? *Diagn Interv Radiol* 2011;17:243-8.
 27. Katahira K, Takahara T, Kwee TC, Oda S, Suzuki Y, Morishita S, et al. Ultra-high-b-value diffusion-weighted MR imaging for the detection of prostate cancer: evaluation in 201 cases with histopathological correlation. *Eur Radiol* 2011;21:188-96.
 28. Kajihara H, Hayashida Y, Murakami R, Katahira K, Nishimura R, Hamada Y, et al. Usefulness of diffusion-weighted imaging in the localization of prostate cancer. *Int J Radiat Oncol Biol Phys* 2009;74:399-403.
 29. Tamada T, Sone T, Jo Y, Tshimitsu S, Yamashita T, Yamamoto A, et al. Apparent diffusion coefficient values in peripheral and transition zones of the prostate: comparison between normal and malignant prostatic tissues and correlation with histologic grade. *J Magn Reson Imaging* 2008;28:720-6.
 30. Ren J, Huan Y, Wang H, Zhao H, Ge Y, Chang Y, et al. Diffusion-weighted imaging in normal prostate and differential diagnosis of prostate diseases. *Abdom Imaging* 2008;33:724-8.
 31. Kim CK, Park BK, Lee HM, Kwon GY. Value of diffusion-weighted imaging for the prediction of prostate cancer location at 3T using a phased-array coil: preliminary results. *Invest Radiol* 2007;42:842-7.
 32. Haider MA, van der Kwast TH, Tanguay J, Evans AJ, Hashmi AT, Lockwood G, et al. Combined T2-weighted and diffusion-weighted MRI for localization of prostate cancer. *AJR Am J Roentgenol* 2007;189:323-8.
 33. Kim CK, Park BK, Han JJ, Kang TW, Lee HM. Diffusion-weighted imaging of the prostate at 3 T for differentiation of malignant and benign tissue in transition and peripheral zones: preliminary results. *J Comput Assist Tomogr* 2007;31:449-54.
 34. Pickles MD, Gibbs P, Sreenivas M, Turnbull LW. Diffusion-weighted imaging of normal and malignant prostate tissue at 3.0T. *J Magn Reson Imaging* 2006;23:130-4.
 35. Nasu K, Kuroki Y, Kuroki S, Murakami K, Nawano S, Moriyama N. Diffusion-weighted single shot echo planar imaging of colorectal cancer using a sensitivity-encoding technique. *Jpn J Clin Oncol* 2004;34:620-6.
 36. Hosseinzadeh K, Schwarz SD. Endorectal diffusion-weighted imaging in prostate cancer to differentiate malignant and benign peripheral zone tissue. *J Magn Reson Imaging* 2004;20:654-61.
 37. Piana G, Trinquart L, Meskine N, Barrau V, Beers BV, Vilgrain V. New MR imaging criteria with a diffusion-weighted sequence for the diagnosis of hepatocellular carcinoma in chronic liver diseases. *J Hepatol* 2011;55:126-32.
 38. Xu PJ, Yan FH, Wang JH, Shan Y, Ji Y, Chen CZ. Contribu-

- tion of diffusion-weighted magnetic resonance imaging in the characterization of hepatocellular carcinomas and dysplastic nodules in cirrhotic liver. *J Comput Assist Tomogr* 2010;34:506-12.
39. Xu PJ, Yan FH, Wang JH, Lin J, Ji Y. Added value of breath-hold diffusion-weighted MRI in detection of small hepatocellular carcinoma lesions compared with dynamic contrast-enhanced MRI alone using receiver operating characteristic curve analysis. *J Magn Reson Imaging* 2009;29:341-9.
 40. Zhang Y, Zhao J, Guo D, Zhong W, Ran L. Evaluation of short-term response of high intensity focused ultrasound ablation for primary hepatic carcinoma: utility of contrast-enhanced MRI and diffusion-weighted imaging. *Eur J Radiol* 2011;79:347-52.
 41. Levy A, Caramella C, Chargari C, Medjhouli A, Rey A, Zareski E, et al. Accuracy of diffusion-weighted echoplanar MR imaging and ADC mapping in the evaluation of residual cervical carcinoma after radiation therapy. *Gynecol Oncol* 2011;123:110-5.
 42. Lambregts DM, Vandecaveye V, Barbaro B, Bakers FC, Lambrecht M, Maas M, et al. Diffusion-weighted MRI for selection of complete responders after chemoradiation for locally advanced rectal cancer: a multicenter study. *Ann Surg Oncol* 2011;18:2224-31.
 43. Song I, Kim CK, Park BK, Park W. Assessment of response to radiotherapy for prostate cancer: value of diffusion-weighted MRI at 3 T. *AJR Am J Roentgenol* 2010;194:W477-82.
 44. Yoshida S, Koga F, Kawakami S, Ishii C, Tanaka H, Numao N, et al. Initial experience of diffusion-weighted magnetic resonance imaging to assess therapeutic response to induction chemoradiotherapy against muscle-invasive bladder cancer. *Urology* 2010;75:387-91.
 45. Eccles CL, Haider EA, Haider MA, Fung S, Lockwood G, Dawson LA. Change in diffusion weighted MRI during liver cancer radiotherapy: preliminary observations. *Acta Oncol* 2009;48:1034-43.
 46. Naganawa S, Sato C, Kumada H, Ishigaki T, Miura S, Takizawa O. Apparent diffusion coefficient in cervical cancer of the uterus: comparison with the normal uterine cervix. *Eur Radiol* 2005;15:71-8.
 47. Namimoto T, Awai K, Nakaura T, Yanaga Y, Hirai T, Yamashita Y. Role of diffusion-weighted imaging in the diagnosis of gynecological diseases. *Eur Radiol* 2009;19:745-60.
 48. Sugita R, Ito K, Fujita N, Takahashi S. Diffusion-weighted MRI in abdominal oncology: clinical applications. *World J Gastroenterol* 2010;16:832-6.
 49. Tamai K, Koyama T, Saga T, Umeoka S, Mikami Y, Fujii S, et al. Diffusion-weighted MR imaging of uterine endometrial cancer. *J Magn Reson Imaging* 2007;26:682-7.
 50. Kyriazi S, Collins DJ, Morgan VA, Giles SL, deSouza NM. Diffusion-weighted imaging of peritoneal disease for noninvasive staging of advanced ovarian cancer. *Radiographics* 2010;30:1269-85.
 51. Kido A, Kataoka M, Koyama T, Yamamoto A, Saga T, Togashi K. Changes in apparent diffusion coefficients in the normal uterus during different phases of the menstrual cycle. *Br J Radiol* 2010;83:524-8.
 52. Feuerlein S, Pauls S, Juchems MS, Stuber T, Hoffmann MH, Brambs HJ, et al. Pitfalls in abdominal diffusion-weighted imaging: how predictive is restricted water diffusion for malignancy. *AJR Am J Roentgenol* 2009;193:1070-6.
 53. Qayyum A. Diffusion-weighted imaging in the abdomen and pelvis: concepts and applications. *Radiographics* 2009;29:1797-810.
 54. McVeigh PZ, Syed AM, Milosevic M, Fyles A, Haider MA. Diffusion-weighted MRI in cervical cancer. *Eur Radiol* 2008;18:1058-64.
 55. Liu Y, Bai R, Sun H, Liu H, Wang D. Diffusion-weighted magnetic resonance imaging of uterine cervical cancer. *J Comput Assist Tomogr* 2009;33:858-62.
 56. Fujii S, Matsusue E, Kanasaki Y, Kanamori Y, Nakanishi J, Sugihara S, et al. Detection of peritoneal dissemination in gynecological malignancy: evaluation by diffusion-weighted MR imaging. *Eur Radiol* 2008;18:18-23.
 57. Low RN, Sebrechts CP, Barone RM, Muller W. Diffusion-weighted MRI of peritoneal tumors: comparison with conventional MRI and surgical and histopathologic findings—a feasibility study. *AJR Am J Roentgenol* 2009;193:461-70.
 58. Shinya S, Sasaki T, Nakagawa Y, Guiquing Z, Yamamoto F, Yamashita Y. The usefulness of diffusion-weighted imaging (DWI) for the detection of gastric cancer. *Hepatogastroenterology* 2007;54:1378-81.
 59. Roy C, Bierry G, Matau A, Bazille G, Pasquali R. Value of diffusion-weighted imaging to detect small malignant pelvic lymph nodes at 3 T. *Eur Radiol* 2010;20:1803-11.
 60. Mir N, Sohaib SA, Collins D, Koh DM. Fusion of high b-value diffusion-weighted and T2-weighted MR images improves identification of lymph nodes in the pelvis. *J Med Imaging Radiat Oncol* 2010;54:358-64.
 61. Kim JK, Kim KA, Park BW, Kim N, Cho KS. Feasibility of diffusion-weighted imaging in the differentiation of metastatic from nonmetastatic lymph nodes: early experience. *J Magn Reson Imaging* 2008;28:714-9.
 62. Chen YB, Liao J, Xie R, Chen GL, Chen G. Discrimination of metastatic from hyperplastic pelvic lymph nodes in patients with cervical cancer by diffusion-weighted magnetic resonance imaging. *Abdom Imaging* 2011;36:

- 102-9.
63. Rockall AG, Sohaib SA, Harisinghani MG, Babar SA, Singh N, Jeyarajah AR, et al. Diagnostic performance of nano-particle-enhanced magnetic resonance imaging in the diagnosis of lymph node metastases in patients with endometrial and cervical cancer. *J Clin Oncol* 2005;23:2813-21.
 64. Torabi M, Aquino SL, Harisinghani MG. Current concepts in lymph node imaging. *J Nucl Med* 2004;45:1509-18.
 65. Lin G, Ho KC, Wang JJ, Ng KK, Wai YY, Chen YT, et al. Detection of lymph node metastasis in cervical and uterine cancers by diffusion-weighted magnetic resonance imaging at 3T. *J Magn Reson Imaging* 2008;28:128-35.
 66. Park SO, Kim JK, Kim KA, Park BW, Kim N, Cho G, et al. Relative apparent diffusion coefficient: determination of reference site and validation of benefit for detecting metastatic lymph nodes in uterine cervical cancer. *J Magn Reson Imaging* 2009;29:383-90.
 67. Sumi M, Sakihama N, Sumi T, Morikawa M, Uetani M, Kabasawa H, et al. Discrimination of metastatic cervical lymph nodes with diffusion-weighted MR imaging in patients with head and neck cancer. *AJNR Am J Neuroradiol* 2003;24:1627-34.
 68. Nakai G, Matsuki M, Inada Y, Tatsugami F, Tanikake M, Narabayashi I, et al. Detection and evaluation of pelvic lymph nodes in patients with gynecologic malignancies using body diffusion-weighted magnetic resonance imaging. *J Comput Assist Tomogr* 2008;32:764-8.
 69. Takahara T, Imai Y, Yamashita T, Yasuda S, Nasu S, Van Cauteren M. Diffusion weighted whole body imaging with background body signal suppression (DWIBS): technical improvement using free breathing, STIR and high resolution 3D display. *Radiat Med* 2004;22:275-82.
 70. Fasih N, Prasad Shanbhogue AK, Macdonald DB, Fraser-Hill MA, Papadatos D, Kielar AZ, et al. Leiomyomas beyond the uterus: unusual locations, rare manifestations. *Radiographics* 2008;28:1931-48.
 71. Tamai K, Koyama T, Saga T, Morisawa N, Fujimoto K, Mikami Y, et al. The utility of diffusion-weighted MR imaging for differentiating uterine sarcomas from benign leiomyomas. *Eur Radiol* 2008;18:723-30.
 72. Hricak H, Chen M, Coakley FV, Kinkel K, Yu KK, Sica G, et al. Complex adnexal masses: detection and characterization with MR imaging--multivariate analysis. *Radiology* 2000;214:39-46.
 73. Thomassin-Naggara I, Toussaint I, Perrot N, Rouzier R, Cuenod CA, Bazot M, et al. Characterization of complex adnexal masses: value of adding perfusion- and diffusion-weighted MR imaging to conventional MR imaging. *Radiology* 2011;258:793-803.
 74. Thomassin-Naggara I, Darai E, Cuenod CA, Fournier L, Toussaint I, Marsault C, et al. Contribution of diffusion-weighted MR imaging for predicting benignity of complex adnexal masses. *Eur Radiol* 2009;19:1544-52.
 75. Takeuchi M, Matsuzaki K, Nishitani H. Diffusion-weighted magnetic resonance imaging of ovarian tumors: differentiation of benign and malignant solid components of ovarian masses. *J Comput Assist Tomogr* 2010;34:173-6.
 76. Nakayama T, Yoshimitsu K, Irie H, Aibe H, Tajima T, Nishie A, et al. Diffusion-weighted echo-planar MR imaging and ADC mapping in the differential diagnosis of ovarian cystic masses: usefulness of detecting keratinoid substances in mature cystic teratomas. *J Magn Reson Imaging* 2005;22:271-8.
 77. Katayama M, Masui T, Kobayashi S, Ito T, Sakahara H, Nozaki A, et al. Diffusion-weighted echo planar imaging of ovarian tumors: is it useful to measure apparent diffusion coefficients? *J Comput Assist Tomogr* 2002;26:250-6.
 78. Hamstra DA, Rehemtulla A, Ross BD. Diffusion magnetic resonance imaging: a biomarker for treatment response in oncology. *J Clin Oncol* 2007;25:4104-9.
 79. Liu Y, Bai R, Sun H, Liu H, Zhao X, Li Y. Diffusion-weighted imaging in predicting and monitoring the response of uterine cervical cancer to combined chemoradiation. *Clin Radiol* 2009;64:1067-74.
 80. Kyriazi S, Collins DJ, Messiou C, Pennert K, Davidson RL, Giles SL, et al. Metastatic ovarian and primary peritoneal cancer: assessing chemotherapy response with diffusion-weighted MR imaging--value of histogram analysis of apparent diffusion coefficients. *Radiology* 2011;261:182-92.
 81. Armitage PA, Schwindack C, Bastin ME, Whittle IR. Quantitative assessment of intracranial tumor response to dexamethasone using diffusion, perfusion and permeability magnetic resonance imaging. *Magn Reson Imaging* 2007;25:303-10.
 82. Rhee TK, Naik NK, Deng J, Atassi B, Mulcahy MF, Kulik LM, et al. Tumor response after yttrium-90 radioembolization for hepatocellular carcinoma: comparison of diffusion-weighted functional MR imaging with anatomic MR imaging. *J Vasc Interv Radiol* 2008;19:1180-6.
 83. Sharma U, Danishad KK, Seenu V, Jagannathan NR. Longitudinal study of the assessment by MRI and diffusion-weighted imaging of tumor response in patients with locally advanced breast cancer undergoing neoadjuvant chemotherapy. *NMR Biomed* 2009;22:104-13.

84. Chen CY, Li CW, Kuo YT, Jaw TS, Wu DK, Jao JC, et al. Early response of hepatocellular carcinoma to transcatheter arterial chemoembolization: choline levels and MR diffusion constants--initial experience. *Radiology* 2006;239:448-56.
85. Cui Y, Zhang XP, Sun YS, Tang L, Shen L. Apparent diffusion coefficient: potential imaging biomarker for prediction and early detection of response to chemotherapy in hepatic metastases. *Radiology* 2008;248:894-900.
86. Harry VN, Semple SI, Gilbert FJ, Parkin DE. Diffusion-weighted magnetic resonance imaging in the early detection of response to chemoradiation in cervical cancer. *Gynecol Oncol* 2008;111:213-20.
87. Koh DM, Scurr E, Collins D, Kanber B, Norman A, Leach MO, et al. Predicting response of colorectal hepatic metastasis: value of pretreatment apparent diffusion coefficients. *AJR Am J Roentgenol* 2007;188:1001-8.
88. DeVries AF, Kremser C, Hein PA, Griebel J, Krezcy A, Ofner D, et al. Tumor microcirculation and diffusion predict therapy outcome for primary rectal carcinoma. *Int J Radiat Oncol Biol Phys* 2003;56:958-65.
89. Dzik-Jurasz A, Domenig C, George M, Wolber J, Padhani A, Brown G, et al. Diffusion MRI for prediction of response of rectal cancer to chemoradiation. *Lancet* 2002;360:307-8.
90. Kwee TC, Takahara T, Ochiai R, Nievelstein RA, Luijten PR. Diffusion-weighted whole-body imaging with background body signal suppression (DWIBS): features and potential applications in oncology. *Eur Radiol* 2008;18:1937-52.
91. Ho KC, Lin G, Wang JJ, Lai CH, Chang CJ, Yen TC. Correlation of apparent diffusion coefficients measured by 3T diffusion-weighted MRI and SUV from FDG PET/CT in primary cervical cancer. *Eur J Nucl Med Mol Imaging* 2009;36:200-8.
92. Komori T, Narabayashi I, Matsumura K, Matsuki M, Akagi H, Ogura Y, et al. 2-[Fluorine-18]-fluoro-2-deoxy-D-glucose positron emission tomography/computed tomography versus whole-body diffusion-weighted MRI for detection of malignant lesions: initial experience. *Ann Nucl Med* 2007;21:209-15.
93. Satoh Y, Ichikawa T, Motosugi U, Kimura K, Sou H, Sano K, et al. Diagnosis of peritoneal dissemination: comparison of 18F-FDG PET/CT, diffusion-weighted MRI, and contrast-enhanced MDCT. *AJR Am J Roentgenol* 2011;196:447-53.
94. Takeshita T, Ninoi T, Doh K, Hashimoto S, Inoue Y. Diffusion-weighted magnetic resonance imaging in tubo-ovarian abscess: a case report. *Osaka City Med J* 2009;55:109-14.
95. Moteki T, Ishizaka H. Diffusion-weighted EPI of cystic ovarian lesions: evaluation of cystic contents using apparent diffusion coefficients. *J Magn Reson Imaging* 2000;12:1014-9.
96. Busard MP, Mijatovic V, van Kuijk C, Pieters-van den Bos IC, Hompes PG, van Waesberghe JH. Magnetic resonance imaging in the evaluation of (deep infiltrating) endometriosis: the value of diffusion-weighted imaging. *J Magn Reson Imaging* 2010;31:1117-23.
97. Oussalah A, Laurent V, Bruot O, Bressenot A, Bigard MA, Regent D, et al. Diffusion-weighted magnetic resonance without bowel preparation for detecting colonic inflammation in inflammatory bowel disease. *Gut* 2010;59:1056-65.